HEAT LOSS IN THE CHANNEL OF A PLASMATRON

L. N. Panasenko

UDC 537.523.5

A mathematical model is constructed and a computational experiment is carried out to determine the characteristics of a longitudinally blown electric arc in the channel of a plasmatron under conditions of local thermal equilibrium. A feature of the model is that it makes allowance for radiation transfer in the real spectrum of an electric-arc plasma. An algorithm for solving the problem is presented and the effect of radiation reabsorption on the radiation and conductive heat loss in the plasmatron channel is shown.

Analysis of studies [1, 2], in which an electric arc is modeled on the basis of the Navier-Stokes equations, showed that the differences between the results calculated from these models and those obtained with the boundary-layer approximation are significant only at distances of roughly the order of 0.5 caliber from the cathode. Excluding this region from discussion, we can model a longitudinally blown electric arc in a channel on the basis of the boundary-layer approximation since it is very simple to find the solution in this case.

To obtain quantitative agreement with experiment, in the initial stage it is most essential, first, to include the radiation transfer in the real spectrum of the electric-arc plasma and, second, to make allowance for the deviation from the local thermal equilibrium (LTE). The region of disruption of the LTE in an electric-arc argon plasma was specified in [3] in calculations of the characteristics of an arc on the basis of the two-temperature model. The current operating conditions of plasmatrons with a linear scheme (high pressure, large channel diameters, high currents, and high gas flow rates) increase the role of collision and radiation processes of energy transfer, which results in LTE virtually over the entire cross section of the channel. In this case, using a cylindrical coordinate system, where the z axis coincides with the axis of symmetry of the channel, we model a laminar electric arc by means of the following system of magnetogasdynamic equations in the boundary-layer approximation:

$$\rho c_p V_z \frac{\partial T}{\partial z} + \rho c_p V_r \frac{\partial T}{\partial r} = \frac{1}{r} \frac{\partial}{\partial r} \left(r\lambda \frac{\partial T}{\partial r} \right) + \sigma E^2 - \nabla \mathbf{q} + V_z \frac{\partial P}{\partial z}, \tag{1}$$

$$\rho V_z \frac{\partial V_z}{\partial z} + \rho V_r \frac{\partial V_z}{\partial r} = \frac{1}{r} \frac{\partial}{\partial r} \left(r\mu \frac{\partial V_z}{\partial r} \right) - \frac{\partial P}{\partial z}, \tag{2}$$

$$\frac{\partial (r\rho V_z)}{\partial z} + \frac{\partial (\rho r V_r)}{\partial r} = 0, \tag{3}$$

$$I = 2\pi E \int_0^R \sigma r dr, \tag{4}$$

$$G = 2\pi \int_0^R \rho V_z r dr. \tag{5}$$

We did not take near-electrode processes and the self-magnetic field into account when constructing the model since they are significant only near the cathode, where the boundary-value approximation is invalid. To solve Eqs. (1) and (2) we must assign one "initial" condition with respect to the z coordinate and two boundary conditions with respect to the radius. In setting these conditions we assumed that the plasma near the cathode and at the channel wall is in equilibrium with them. As the initial profile we used the parabolic profile

$$T(r, 0) = T_c \left[1 - \left(\frac{r}{R} \right)^2 \right] + T_w. \tag{6}$$

A. V. Lykov Institute of Heat and Mass Transfer, Academy of Sciences of the Belorussian SSR, Minsk. Translated from Inzhenerno-Fizicheskii Zhurnal, Vol. 58, No. 3, pp. 505-511, March, 1990. Original article submitted December 29, 1988.

 0022-0841/90/5803-0376$12.50

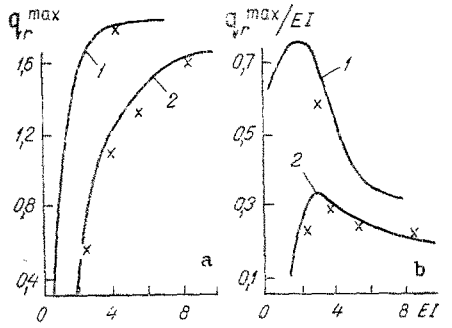

Fig. 1

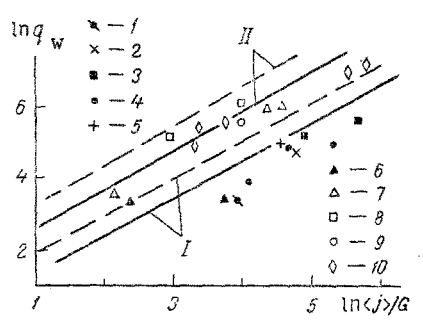

Fig. 2

Fig. 1. Radiation of a column of arc: a) I maximum radiation heat flow q_r (kW/cm) of a unit column of arc versus the discharge power EI (kW/cm) in argon (1) and in air (2); b) relative radiation of an argon (1) and air (2) electric-arc plasma; the points indicate experimental data [3].

Fig. 2. Heat loss ln q_w (W/cm^2) in the steady-state segment, as a function of the determining parameters ln ⟨j⟩/G, kA·sec/cm^2·kg: I) argon; 1) experimental data [13], 2) [21], 3) [22], 4) [23], 5) [24], 6) [25]; II) air; 7) experimental data [13], 8) [19], 9) [26], 10 [27]; the dashed curves take the radiation into account in the bulk luminescence approximation.

The constant T_c models the conditions at the cathode: according to [4], the temperature in the spot does not exceed 5000 K. The temperature of the cooled wall is $T_w \simeq 300$ K. The initial velocity distribution was assigned by using the condition of constant gas flow rate (5):

$$V_z(r,\ 0) = G\left[1 - \left(\frac{r}{R}\right)^2\right] / 2\pi \int_0^R \rho r \left[1 - \left(\frac{r}{R}\right)^2\right] dr. \tag{7}$$

As the boundary conditions with respect to the radius we use the symmetry conditions at r = 0

$$\frac{\partial T(0,\ z)}{\partial r} = 0; \quad \frac{\partial V_z(0,\ z)}{\partial r} = 0 \tag{8}$$

and the conditions at the wall at r = R

$$T(R,\ z) = T_w; \quad V_z(R,\ z) = 0. \tag{9}$$

The continuity equation (3) was used to determine the radial velocity component with the boundary condition on the axis

$$V_r(0,\ z) = 0. \tag{10}$$

The characteristics of the electric-arc discharge in streams of argon and air were calculated with given functions $\sigma(T, P)$, $\rho(T, P)$, $\lambda(T, P)$, and $c_p(T, P)$ from known sources in the literature. The density and heat capacity of an argon plasma in the range 1000 K ≤ T ≤ 20,000 K at P = 0.1 MPa are given in [5, 6] and the thermal conductivity and electrical conductivity are given in [7]. The analogous data for an air plasma were taken from [8, 9]. The divergence ∇q of the radiation flux in the real spectrum of an electric-arc plasma was determined on the basis of the method of partial characteristics, whose application in the calculation of the characteristics of electric arcs was described in [10].

The flow version of the difference factorization method [11] was used to solve the problem, since it ensures that stable convergent conditions are obtained under abrupt changes (by several orders of magnitude) in the coefficients in equations of the form

$$a\frac{\partial u}{\partial z} + c\frac{\partial u}{\partial r} = \frac{1}{r}\frac{\partial}{\partial r}\left(rb\frac{\partial u}{\partial r}\right) + d. \tag{11}$$

The difference scheme in the computational region (half the longitudinal section of the channel) was constructed by introducing two grids: with integer nodes $r_i = n_i\Delta r$, $z^j = m^j\Delta z$ and with half-integer nodes $r_{i+1/2} = \sqrt{(r_{i+1}^2 + r_i^2)/2}$, $z^{j+1/2} = (z^{j+1} + z^j)/2$. When determining the flows $W = -b\partial u/\partial r$ at integer nodes and the functions u and coefficients a, b, c, d at half-integer nodes we replaced the derivatives of equations of the type (11) with finite differences. Recasting the difference analog of Eq. (11) to the form

$$A_{i+1/2}\,W_i^{j+1} - B_{i+1/2}W_{i+1}^{j+1} - C_{i+1/2}\,u_{i+1/2}^{j+1} = -F_{i+1/2} \tag{12}$$

and following the procedure of [11] for obtaining the recurrence relations for the difference-factorization coefficients α_i, β_i, γ_i (forward difference factorization: i = 0, 1, ..., N − 1) in the relation between the unknown function and its flux

$$\alpha_i u_{i+1/2} + \beta_i W_i = \gamma_i, \tag{13}$$

we can determine by reverse difference factorization (i = N − 1, ..., 1, 0)

$$W_i^{j+1} = \frac{1}{A_{i+1/2}}\left[\left(1 - \frac{C_{i+1/2}}{A_{i+1/2}}\,\beta_i\right)(B_{i+1/2}\,W_{i+1}^{j+1} - F_{i+1/2}) + C_{i+1/2}\,\gamma_i\right], \tag{14}$$

$$u_{i+1/2}^{j+1} = \frac{1}{A_{i+1/2}}\,[A_{i+1/2}\,\gamma_i + \beta_i\,(F_{i+1/2} - B_{i+1/2}\,W_{i+1}^{j+1})]. \tag{15}$$

The value of the flow W_N was found from the boundary condition at the wall and the linear relation (13) at the point i = N. The algorithm for the solution of the problem envisaged the organization of inner iterations (with respect to nonlinearity), intermediate iterations (for the link between the equations), and outer iterations (to refine the pressure in the initial cross section of the channel). The condition for the convergence of inner iterations

$$|1 - u_{i+1/2}^{(s+1)}/u_{i+1/2}^{(s)}| < \varepsilon, \quad i = 0,\ 1,\ \ldots,\ N-1, \tag{16}$$

at a given $\varepsilon = 0.1$ made it possible to obtain a solution in the calculated layer to within 10%.

The solution of the equation of motion differed from the solution of the energy transfer equation because of the indeterminacy of $\partial P/\partial z$ [the source term in the corresponding equation (11)]. The equation of motion, therefore, was solved by the method of [12], making it possible to obviate this difficulty by means of the representation

$$V_z = \xi + \omega\,\frac{\partial P}{\partial z}\,. \tag{17}$$

In order to use the formulas of the flow version of the difference factorization method to solve the equation of motion as well, this method was modified by introducing a representation of type (17) for the flow

$$W_{i+1} = L_{i+1} + M_{i+1}\,\frac{\partial P}{\partial z}\,. \tag{18}$$

As a result we obtain two difference schemes: the first for determining L_{i+1}^{j+1}, $\xi_{i+1/2}^{j+1}$:

$$\begin{gathered} A_{i+1/2}\,L_i^{j+1} - B_{i+1/2}L_{i+1}^{j+1} - C_{i+1/2}\,\xi_{i+1/2}^{j+1} = -F_{i+1/2}\,, \\ L_{i+1}^{j+1} = -\tilde{b}_{i+1}^{j+1}\,(\xi_{i+3/2}^{j+1} - \xi_{i+1/2}^{j+1}), \quad \tilde{b}_{i+1}^{j+1} = b_{i+1}^{j+1}/(r_{i+3/2} - r_{i+1/2}) \end{gathered} \tag{19}$$

with a given boundary condition and the second for determining M_{i+1}^{j+1}, $\omega_{i+1/2}^{j+1}$,

$$\begin{gathered} A_{i+1/2}\,M_i^{j+1} - B_{i+1/2}M_{i+1}^{j+1} - C_{i+1/2}\omega_{i+1/2}^{j+1} = -E_{i+1/2}\,, \\ M_{i+1}^{j+1} = -\tilde{b}^{\,j+1}_{i+1}\,(\omega_{i+3/2}^{j+1} - \omega_{i+1/2}^{j+1}) \end{gathered} \tag{20}$$

with zero boundary condition. After solving these systems from the formulas of the flow version of the difference factorization method we determined

$$\left(\frac{\partial P}{\partial z}\right)^{j+1} = \frac{G}{\pi} - \frac{\sum_{i=0}^{N-1} [(r\rho\xi)_{i+1/2} + (r\rho\xi)_{i+3/2}] (r_{i+3/2} - r_{i+1/2})}{\sum_{i=0}^{N-1} [(r\rho\omega)_{i+1/2} + (r\rho\omega)_{i+3/2}] (r_{i+3/2} - r_{i+1/2})} \quad (21)$$

and the distribution of the velocity V_z^{j+1} in accordance with representation (17).

By solving system (1)-(5) we determined the following characteristics of an electric-arc plasma: temperature distribution T(r, z) and velocity distributions $V_z(r, z)$ and $V_r(r, z)$ in the channel, the specific mass flow rate of the gas, the electric field strength, the axial and radial components of the convective, conductive, and radiation heat flows, the heat flows in the channel wall, the mean-mass enthalpies, pressure variation along the length of the channel, and the specific radiation power at each computational point. We studied the following ranges of determining parameters for arcs in an air flow: I = 50-500 A, G = (1-4)·10^{-3} kg/sec, R = 0.5 and 1 cm, and L = 10 and 50 cm. The characteristics of an argon arc for the same values of R and L were calculated at I = 10-200 A and G = (0.3-3)·10^{-3} kg/sec. A pressure P = 0.1 MPa was assigned at the channel exit.

Analysis of the calculated results revealed that radiation reabsorption has a stronger effect on the thermal characteristics of an arc than on its electrical and gasdynamic characteristics [10]. Here we have presented in detail the thermal characteristics, in particular the heat loss in the channel, with radiation and conductive heat flows in the wall as its components.

The axial temperature of a plasma with allowance for the radiation transfer in the real spectrum decreased by 500-2000 K in comparison with the bulk-radiation approximation while the temperature rose by 1000-2000 K at the wall. Heating of the boundary layers during radiation reabsorption reduced the heat flows in the wall, which determine the heat losses in the plasmatron channel. For some computational variants this decrease amounted to 50% and led to quantitative agreement between the calculated heat losses and the experimental data.

In the initial segment of the arc the main contribution to the heat loss is made by radiation and the conductive flow is insignificant. The radiation loss in this segment for an air electric-arc plasma is less than for an argon plasma at the same discharge power (Fig. 1a). As the arc power in argon increases from 2 to 4 kW/cm the radiation of a unit column of arc in air increases sharply. At high powers the increase in radiation slows down and the fraction of radiation in the energy balance decreases with rising discharge power. As a result the relative magnitude of the radiation depends nonmonotonically on the arc power (Fig. 1b): first it increases, reaching 75% of the power input for an argon plasma and 35% for an air plasma, and then decreases to 30 and 20%, respectively. In the limit the radiation in a high-temperature plasma is only a few per cent of the power input. Many photoprocesses leading to the formation of a line spectrum are absent from a completely ionized simple plasma, such as a high-temperature plasma. In this case the main role is played by electron brehmsstrahlung. Studies of such a plasma began much earlier than that of a partially ionized plasma. The attempts to calculate the characteristics of electric arcs without allowance for radiation probably stemmed from an unsubstantiated transfer of the results of these studies to the case of a partially ionized electric-arc plasma.

In order to evaluate the advantages of this model as well as the reliability of the calculations, we compared the obtained thermal characteristics on the steady-state segment of an arc with experimental data in the literature. The thermal characteristics as functions of each of the determining parameters I, G, R with the other two fixed often cannot be compared directly because of the lack of a broad set of experimental data. All the variants of the calculation of the thermal characteristics, therefore, were processed as dependences on dimensional complexes, consisting of the determining parameters I, G, R. For comparison we selected those experiments in which the values of the complexes $\langle j\rangle G$ and $\langle j\rangle/G$, where $\langle j\rangle = I/\pi R^2$, fell within the ranges studied in the calculations. In the steady-state part of the arc, therefore, we made a comparison with experiment for the heat loss, axial temperatures, and mean-mass enthalpies. The conductive heat flows in the channel wall in this range are comparable to the radiation loss and amount to heat loss which increases with the channel radius and gas flow rate (Fig. 2). For an arc burning in an air flow the calculated heat loss is in better agreement with the experimental values than for an argon plasma. In the case of an arc in an argon flow we obtain overestimated heat flows in the wall also with allowance for radiation reabsorption. The deviation in some variants reaches 30% for an argon plasma and 10% for an air plasma. The main cause of this deviation rests in the considerable spread of the experimental data as well as in the imperfection of the model used. The point is that because of the instability of the arcing and the diversity of the designs we cannot expect the experimental data of different authors to be in agreement. Moreover, the proposed model of an arc does not make allowance for physical phenomena that occur at the channel wall (e.g., turbulization of the flow and the nonequilibrium of the plasma at the wall, shunting, and breakdown). Nevertheless, from Fig. 2 we see that inclusion of radiation reabsorption allows more reliable arc characteristics to be obtained.

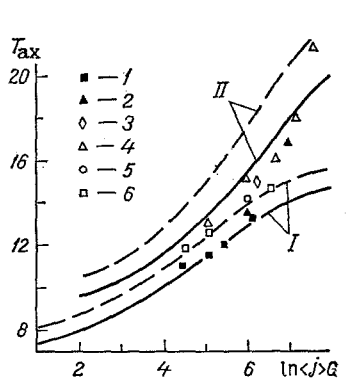

Fig. 3

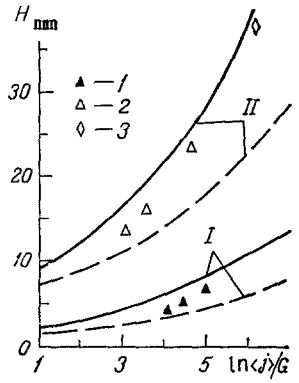

Fig. 4

Fig. 3. Axial temperature T_{ax} (10^3 K) in the steady-state segment of the arc as a function of the determining parameters in ⟨j⟩G, mA·kg/cm²·sec: I) argon; 1) experimental data [14], 2) [15]; II) air; 3) experimental data [14], 4) [16], 5) [17], 6) [18]; the dashed curves takes the radiation into account in the bulk luminescence approximation.

Fig. 4. Mean-mass enthalpy H_{mm} (mJ/kg) as a function of the determining parameters ln ⟨j⟩/G, kA·sec/cm²·kg: I) argon; 1) experimental data [19]; II) air; 2) experimental data [19], 3) [20]; the dashed curves take the radiation into account in the bulk luminescence approximation.

In accordance with large radiation heat loss the axial values of the temperatures for an arc in an argon flow are slightly lower than those in air (Fig. 3). Inclusion of radiation reabsorption leads to lower axial temperatures and good quantitative agreement with experiment. Since the reabsorbed radiation is an additional source heating the plasma, this has a particular effect on the mean-mass enthalpy (Fig. 4). In the investigated ranges of the determining parameters the increase in the mean-mass enthalpy because of radiation reabsorption averages 35% in argon and 30% in air.

Our numerical experiment permits us to make a conclusion not only that the radiation must be taken into account in calculations of the characteristics of an electric-arc plasma but also that it is important to include the radiation reabsorption. Without allowance for radiation reabsorption quantitative agreement cannot be obtained between the calculated and experimental characteristics in the steady state segment of the arc as well as in the initial segment.

NOTATION

Here ρ, c_p, σ, λ, and μ are the density, heat capacity, electrical conductivity, thermal conductivity, and viscosity; V_z and V_r are the velocity components in cylindrical coordinates; T and P are the temperature and pressure; I and E are the electric current and the electric field strength; G is the gas flow rate; R and L are the channel radius and length; and ∇q is the divergence of the radiation flux.

LITERATURE CITED

1. A. N. Prokof'ev, Izv. Vyssh. Uchebn. Zaved, Mashinostroenie, No. 3, 81 (1977).
2. A. S. Korneev, Abstracts of Papers Read at Eighth All-Union Conference on Generators of Low-Temperature Plasma. Part 1 [in Russian], Novosibirsk (1980), pp. 89-92.
3. L. N. Panasenko, and V. G. Sevast'yanenko, Inzh-Fiz. Zh., 52, No. 4, 611 (1987).
4. M. F. Zhukov, A. S. Koroteev, and B. A. Uryukov, Applied Dynamics of Thermal Plasma [in Russian], Novosibirsk (1975).
5. V. P. Glushko (ed.), Thermodynamic Properties of Individual Substances [in Russian], Moscow (1978).
6. N. B. Vargaftik, Handbook of Thermophysical Properties of Gases and Liquids [in Russian], Moscow (1972).
7. R. S. Devoto, Phys. Fluids, 16, No. 5, 616 (1973).
8. A. S. Predvoditelev (ed.), Tables of Thermodynamic Functions of Air [in Russian], Moscow (1962).
9. I. A. Sokolova, Prikl. Mekh. Tekh. Fiz., No. 2, 80 (1973).

10. L. N. Panasenko and V. G. Sevast'yanenko, Inzh.-Fiz. Zh., 48, No. 2, 279 (1985).
11. N. N. Kalitkin, Numerical Methods [in Russian], Moscow (1978).
12. L. M. Simuni, Zh. Vychisl. Mat. Mat. Fiz., 5, No. 6, 1138 (1965).
13. V. P. Lukashov, "Heat exchange and gasdynamics in the discharge channel of an electric-arc gas heater in the initial segment," Author's Abstract of Candidate's Dissertation [in Russian], Novosibirsk (1986).
14. N. F. Aleshin, V. V. Azharonok, G. P. Lizunkov, et al., Problems of Heat and Mass Exchange-86 [in Russian], Minsk (1986), pp. 62-64.
15. V. S. Klubnikin, Low-Temperature Plasma Physics, Technique, and Application: Proceedings of Fourth All-Union Conference on Low-Temperature Plasma Physics and Generators [in Russian], Alma-Ata (1970), pp. 58-62.
16. S. V. Alekseev, A. A. Voropaev, A. V. Donskoi, et al., Low-Temperature Plasma Physics, Technique, and Application: Proceedings of Fourth All-Union Conference on Low-Temperature Plasma Physics and Generators [in Russian], Alma-Ata (1970), pp. 145-148.
17. T. V. Osipova, Low-Temperature Plasma Generators: Proceedings of Third All-Union Conference on Low-Temperature Plasma Generators [in Russian], Moscow (1969), pp. 403-413.
18. V. P. Lukashov, B. A. Pozdnyakov, and N. N. Shcherbik, Ninth All-Union Conference on Low-Temperature Plasma Generators [in Russian], Frunze (1983), pp. 88-89.
19. A. B. Ambrazyavichyus, in: Experimental Plasmatron Studies [in Russian], M. F. Zhukov (ed.), Novosibirsk (1977), pp. 104-119.
20. J. R. Jedlicka and H. A. Stine, IEEE Trans. Nucl. Sci., NS-11, 104 (1964).
21. A. I. Ivlyutin, A. B. Karabut, and Yu. V. Kurochkin, Abstracts of Papers Read at Fifth All-Union Conference on Low-Temperature Plasma Generators, Part 1 [in Russian], Novbosibirsk (1972), pp. 205-207.
22. A. V. Donskoi, V. S. Klubnikin, and A. S. Parkhomenko, Teplofiz. Vys. Temp., No. 3, 486 (1970).
23. N. F. Aleshin, A. F. Bublievskii, and L. N. Panasenko, Processes in Low-Temperature Plasma and Plasma Apparatuses [in Russian], Minsk (1983), pp. 100-107.
24. Yu. V. Kurochkin and A. V. Pustogarov, in: Experimental Plasmatron Studies [in Russian], M. F. Zhukov (ed.), Novosibirsk (1977), pp. 82-104.
25. R. M. Kezhyalis, R. I. Virbaitis, A. I. Shilkov, et al., Tr. Akad. Nauk Lit. SSR, Ser. B, 1 (116), 69 (1980).
26. I. M. Zasypkin and É. K. Urbakh, Ninth All-Union Conference on Low-Temperature Plasma Generators [in Russian], Frunze (1983), pp. 74-75.
27. P. G. Vasil'ev, A. V. Donskoi, and V. S. Klubnikin, Low-Temperature Plasma Generators: Abstracts of Papers Read at Tenth All-Union Conference (Kaunas, September 16-18, 1986), Part 1 [in Russian], Minsk (1986), pp. 33-34.